Eur. J. Wood Prod. (2015) 73:199–207
DOI 10.1007/s00107-014-0853-1

ORIGINAL

Effects of zirconaluminate coupling agent on mechanical properties, rheological behavior and thermal stability of bamboo powder/polypropylene foaming composites

Xia Xing Zhou · Yan Yu · Li Hui Chen

Received: 26 November 2013 / Published online: 16 November 2014

Abstract To improve the interfacial adhesion of bamboo powder (BP) and polypropylene (PP), the effects of zirconaluminate coupling agent (TL) on the mechanical properties, rheological behavior and thermal stability of 33 wt% injection moulded BP/PP foaming composites were investigated. The bending and tensile properties were enhanced first as the TL content increased and then decreased as the TL content exceeded 1 %; the notched impact strength improved steadily with increased TL content. The 1 % TL-treated composite showed the best comprehensive mechanical properties; the bending, tensile, and notched impact strengths were increased by 9.0, 9.7, and 16.1 %, respectively; and water absorption for 1,920 h was decreased from 8.85 to 2.61 % compared to the untreated composite. The frequency sweep results indicated that the slope of lgG'–lg$f$ curve increased from 0.709 in the untreated composite to 0.842 in the 1 % TL-treated composite. The TG results revealed that thermal stability was slightly improved in the TL-treated composite. Environmental scanning electron microscopy showed that the interfacial compatibility of the treated composite improved, which was confirmed by Fourier transform infrared spectroscopy and X-ray photoelectron spectroscopy analysis.

X. X. Zhou · L. H. Chen (✉)
College of Material Engineering, Fujian Agriculture and Forestry University, Fuzhou, China
e-mail: lihuichen@263.net

Y. Yu
Department of International Cooperation, International Center for Bamboo and Rattan, Beijing, China

1 Introduction

Wood–plastic composites (WPCs) demonstrate remarkable environmental and economical advantages, and therefore they have a wide application field such as decoration, building, packing, and transportation (Ashori and Nourbakhsh 2011). Additionally, in order to reduce the density, improve the specific strengths and broaden the application fields, foaming technology has been widely used for microcellular WPCs over recent decades (Bledzki et al. 2005; Lee et al. 2011; Zhang et al. 2012).

It is well known that China has the most abundant and under-utilized bamboo resources in the world. Bamboo fiber possesses excellent intrinsic properties including fast growing, low density, high tensile modulus and biodegradability. Bamboo fiber can be a cheaper substitute for synthetic fibers such as glass fiber and carbon fiber in some application fields (Okubo et al. 2004). Due to these outstanding properties, many researchers have focused on the composites reinforced with bamboo fibers (Zhang et al. 2010; Rawi et al. 2013). As a processing residue of bamboo, bamboo powder (BP) can also be used as reinforcement of WPCs.

Polypropylene (PP) is widely used as a major matrix of WPCs because it exhibits higher heat resistance, higher corrosion resistance and easier recycling degradability than polyethylene (PE), and it brings out less environment pollution than polyvinyl chloride (PVC)-based products (Lee et al. 2007). Therefore, in this study BP/PP foaming composites were prepared using an injection molding process. During the last decades, the methods of esterification (Freire et al. 2006) or etherification or benzylation of natural fibers and using coupling agents have been widely applied to improve the compatibility between matrices and fillers (Dominkovics et al. 2007). In PP-based WPCs, the

most common coupling agents are maleinated polypropylene (MAPP) and maleinated polyethylene (MAPE) and silane (Deka and Maji 2010; Xie et al. 2010; Gao et al. 2012; Lou et al. 2013; Yeh et al. 2013). In the 1980s, zirconaluminate (TL) was potentially used as a coupling agent in the plastic, paper, and rubber industry, and also other industries (Cohen 1985; Chen et al. 2006; Tang et al. 2007; Li et al. 2013). TL can also be a useful coupling and hydrophobing agent for cellulosic fiber/flour-polyolefin composites.The bending modulus and toughness in the 30 % wood flour/PP composite at a concentration of 1 % TL were increased by 4.8 and 11.3 %, respectively (Freischmidt and Michell 1991). Moreover, TL can replace silane coupling agent in many cases because it has stronger organic reactivity and can better improve the compatibility of composites (Guo et al. 2011). However, the application of TL to foaming WPCs has been rarely reported and so far it is unknown whether the TL has a positive effect on the mechanical properties, rheological behavior, and thermal stability of WPCs. Therefore, it is significant to systematically study the effects of TL on the properties of PP/BP foaming composites.

2 Materials and methods

2.1 Materials

Moso bamboo (*Phyllostachys edulis*) powder with a mixture of particle sizes in the range of 90–450 μm and a density of 1.37 g/cm^3 was supplied by Zhejiang Lin-an Mingzhu Bamboo and Wood Industry Co., Ltd, China. High melted strength polypropylene (HMSPP), of type SMS-514F, with a density of 0.91 g/cm^3 and melting index (MI) of 3.2 g/10 min (230 °C/2.16 kg) was provided by Korea Honam Petrochemical Ind. Co, Ltd. PP (of type K8303) with a density of 0.90 g/cm^3 and MI of 2.4 g/10 min (230 °C/2.16 kg) was provided by ExxonMobil Chemicals. Modified azodicarbonamide (AC) was used as foaming agent (FA). With the intention of improving the compatibility between the BP, PP, and HMSPP, a zircoaluminate coupling agent (TL) from Chongqing Jiushuo Industry and Trade Co. Ltd, China was used. Five proportions of TL, i.e., 0, 0.5, 1, 2, and 3 % of BP weight were studied in this research.

2.2 Preparation of BP/PP foaming composites

First, the TL coupling agent was added to ethanol at a ratio of 1:4. The bamboo powders were dried and treated using the TL solution in a high-speed Herschel mixer (HM40 KM120) at 80 °C for 15 min. Then the TL-treated BP was oven dried at 80 °C to 1–2 % moisture content. Second, PP, HMSPP, lubricant (stearic and calcium stearate) and the TL-treated BP were mixed in a Herschel mixer for 10 min. Third, the mixture was transferred to a Haake Torque rheometer and mixed at a temperature of 185 °C, at a rotational speed of 40 rpm for 12 min. Then, the blends were crushed into granules in a WSGM-250 mill. Finally, the BP/PP granules and the FA were mixed, and the foaming samples were prepared by injection molding. The PP, HMSPP, BP, lubricant, and FA accounted for 52, 13, 33, 1, and 1 wt% of the foaming composite, respectively, as previously reported (Zhou et al. 2012).

2.3 Mechanical properties

Density of the specimen was measured according to ASTM D-792. Flexural properties in three-point bending mode and tensile strength were determined at a speed of 10 mm/min, and according to ASTM D-790 and ASTM D-638, respectively. The notched impact strength was measured in accordance with EN ISO 179. Each value obtained represented the average of six samples. The specimen dimensions exactly met these standards.

2.4 Water absorption and thickness swelling

Percentage water absorption (WA) and thickness swelling (TS) tests were carried out according to ASTM D570. The specimens had the following dimensions: length of 30 mm, width of 12 mm and thickness of 4 mm. The foaming pallets were immersed in distilled water at 23 °C for 1,920 h. All values were calculated as the mean of four samples. The WA and TS were determined using the following equations:

$$WA = \left(\frac{m_t - m_o}{m_o}\right) \times 100 \quad (1)$$

where m_t is the mass of the sample after water soaking; and m_o is the mass of the sample before water soaking.

$$TS = \left(\frac{T_t - T_o}{T_o}\right) \times 100 \quad (2)$$

where T_t is the thickness of the sample after water soaking; and T_o is the thickness of the sample before water soaking.

2.5 Rheological behavior

Rheological measurements of the samples were performed using a rotational rheometer (Haake ARSIII, Germany). A dynamic frequency sweep test was conducted to measure the storage modulus (G') and complex viscosity (η^*) at a frequency range of 0.1–100 Hz in the linear viscoelastic region at a constant temperature of 180 °C.

2.6 Thermal stability

For thermal gravimetric (TG) analysis, the samples were dried in an oven at 105 °C for 2 h. The thermal decomposition behavior of composites was characterized using a TG-DTA (Netzsch STA449C, Germany) at a heating rate of 10 °C min^{-1} up to 800 °C under nitrogen atmosphere.

2.7 ESEM analysis

The tensile fractured surfaces of untreated and TL-treated composites were investigated by Environmental scanning electron microscopy (ESEM) (XL30 PHILIPS, FET, the Netherlands) after being treated with gold sputtering.

2.8 FTIR studies

Fourier transform infrared spectra (FTIR) of TL, untreated BP, TL-treated BP, untreated BP/PP foaming composite and TL-treated composite were recorded by FTIR (AGL0702005 Nicolet 380, USA) under test conditions of 4 cm^{-1} resolution, scan number of 32, and scan range of 4,000–400 cm^{-1}.

2.9 XPS analysis

Compositions of foaming composites untreated and TL-treated were analyzed by X-ray photoelectron spectroscopy (XPS) (ESCALLAB 250, UK) with a scientific theta probe. The X-ray source was Al Ka (1,486.6 eV) and samples were analyzed at pressures of 2×10^{-10} mbar with a pass energy of 30 eV and energy step size of 0.05 eV. To determine types of oxygen–carbon bonds present, chemical bond analysis of carbon was accomplished by curve fitting of the C1s peak and deconvolution into four sub-peaks. An oxygenated to unoxygenated carbon ratio ($C_{ox/unox}$) was calculated using Eq. (3) (Dorri and Gray 1978):

$$C_{ox/unox} = \frac{C_{oxygenated}}{C_{unoxygenated}} = \frac{C2 + C3 + C4}{C1} \quad (3)$$

3 Results and discussion

3.1 Mechanical properties

Because the TL did not obviously affect the composites' densities, the density curve is not shown in this paper. The densities of foaming composites were all about 0.87 g cm^{-3}, decreased by 14 %, compared to the unfoaming one (Zhou et al. 2012). The mechanical properties of foaming composites treated with different contents of TL are presented in Fig. 1. Evidently, the mechanical properties of TL-treated composites improved compared to those of the untreated analogue. The flexural and tensile strengths were enhanced first and then decreased when the TL content exceeded 1 %. This was because at a moderate TL concentration, the surface wetting and dispersion of BP particles in the matrices were promoted and the interfacial compatibility between BP and matrices was improved, as shown in the ESEM morphology (Fig. 5). However, the excessive TL may form a layer of macromolecules, resulting in the decreased uniformity between the fillers and matrices. The flexural modulus was enhanced significantly with the addition of 1 % TL, but was improved to a less degree by higher TL. The notched impact strength was obviously enhanced with TL content increasing from 0 to 1 %, but then improved steadily with further increasing TL content. It can be concluded that the TL played a positive role in the increased energy absorption during crack propagation. This was because TL improved the interfacial interaction between BP and matrices, leading to increased efficiency of stress transfer from the matrices to the fillers. This finding was consistent with previous studies on other coupling agents such as MAPP (Kim et al. 2007).

3.2 Water absorption and thickness swelling

The time dependence of both water absorption (WA) and thickness swelling (TS) in composites is shown in Fig. 2. The WA and TS of the TL-treated composites were found to decrease drastically. Clearly, the WA and TS of the untreated composite were 8.85 and 1.93 %, respectively, after 1,920 h of immersion time. This could be ascribed to the poor interface between fillers and matrices. As for the 1 % TL-treated composite, the growth trends of WA and TS were significantly weakened, and the WA and TS eventually decreased to constant values of 2.61 and 1.52 %, respectively. These results clearly revealed that the use of TL as coupling agent was proven to benefit the WA and TS of the composites. First, this is due to the improvement in the interfacial compatibility and interfacial bonding between the BP and matrices, and thus the gap between the BP and PP became smaller. Second, the wetting of TL-treated BP by the matrices was more sufficient and the amounts of hygroscopic hydroxyl groups in the BP became less due to their reactions with TL groups, which further contributed to the reduced water uptake. This assumption was supported by ESEM, FTIR and XPS as mentioned below. Additionally, the higher TL content resulted in slightly lower WA and considerably smaller TS. However, it should be mentioned that the water resistance was not improved anymore when the TL content exceeded 2 %.

The optimal amount of TL was assessed to be 1 %, based on a comprehensive consideration of the mechanical

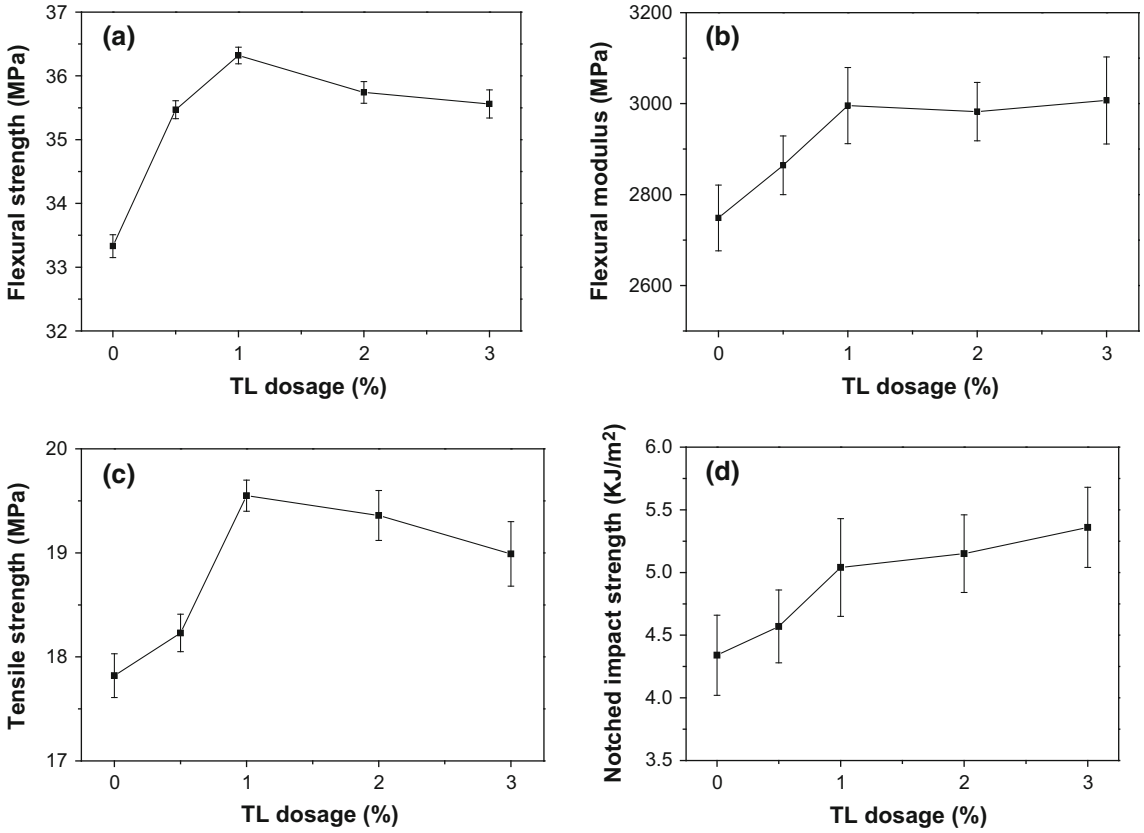

Fig. 1 Effects of TL on the mechanical properties of BP/PP foaming composites

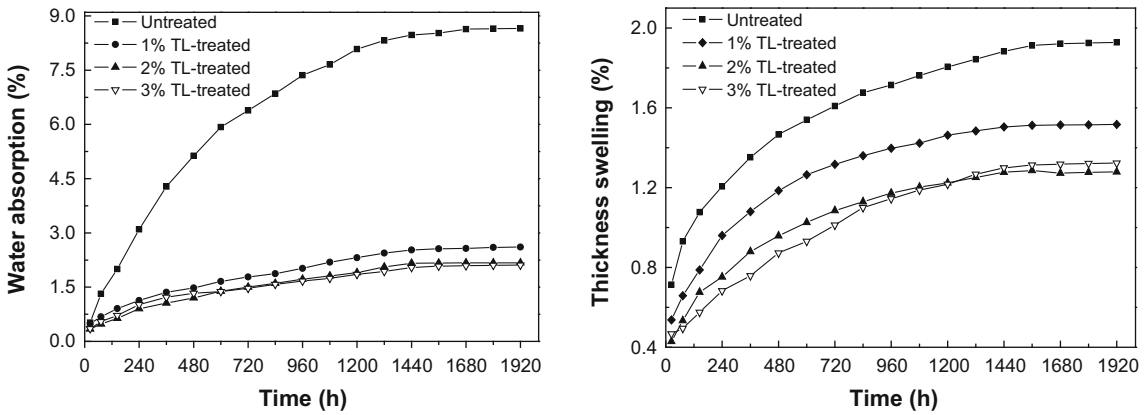

Fig. 2 Effects of TL on the water absorption and thickness swelling of foaming composites

properties, water resistance and the cost of composites. In this case, the mechanical properties with respect to flexural modulus, flexural, tensile, and notched impact strengths were increased to 2,895.78, 36.32, 19.55 MPa, and 5.04 kJ/m^2, respectively, yielding improvements of 9.0, 9.4, 9.7, and 16.1 %, respectively, compared to the untreated composite; the water resistance was improved significantly. Compared with the MAPP-treated wood flour/PP composites (Kim et al. 2007) and MAPP-treated BP/PP foaming composites (Zhou et al. 2013), the improvements of mechanical properties for the TL-treated composites were much lower. However, the optimum content of TL was also much lower than that of MAPP. The mechanical properties such as bending strength and bending modulus, and the water resistance of TL-treated foaming composites meet the requirements of WPC floorings and WPC decorative boards according to GB/T 24508-2009 and GB/T 24137-2009, respectively.

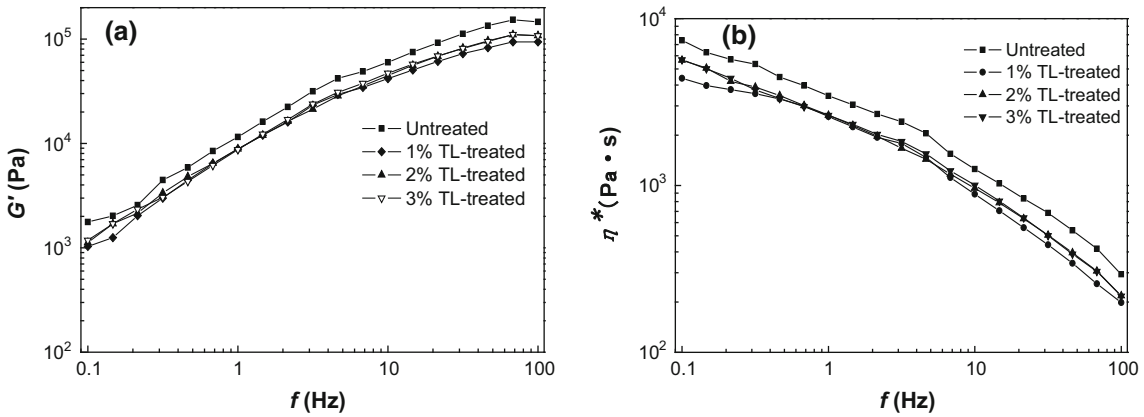

Fig. 3 Dependence of storage modulus (G') and complex viscosity (η^*) on frequency (f) for foaming composites treated with various TL contents at 180 °C

3.3 Rheological behavior

The effects of TL content (0, 1, 2 and 3 %) on the storage modulus (G') and complex viscosity (η^*) as a function of frequency (f) are illustrated in Fig. 3a, b, respectively. Storage modulus was obviously enhanced with increased frequency, especially at low frequency (0.1–20 Hz) and the increasing speed of G' gradually eased at higher frequency (20–100 Hz). Complex viscosity was reduced with increased frequency (Fig. 3b), showing typical shear thinning effect. The viscoelastic response of BP/PP foaming composites varied with TL contents. Compared to the untreated composite, G' and η^* of TL-treated composites were all reduced, indicating that TL promoted the improvement of processing properties.

Available research shows that a higher slope of the lgG'-lg$f$ curve at the terminal region results in greater homogeneous phase in the composite (Gao et al. 2012). Linear fitting of the lgG'-lg$f$ curve at low frequency showed that the slopes of the untreated sample and the samples treated with 1, 2, and 3 % TL were 0.709, 0.842, 0.805, and 0.823, respectively, with coefficients of determination higher than 0.98. Therefore, the results indicated that the degree of homogeneity was a little higher after the addition of TL and the homogeneous degree was the highest in the 1 % TL-treated composite. These results proved that the TL enhanced interaction between the bamboo particle and the polymer matrices. These findings also corresponded to the mechanical measurements.

3.4 Thermal properties

Figure 4 depicts the TG and derivative thermogravimetric (DTG) thermograms of the untreated and 1 % TL-treated composites. Table 1 shows the initial decomposition temperature (T_i), maximum pyrolysis temperature (T_m), decomposition temperature at different weight loss (%) (T_d), maximum weight loss rate (W_m) and residual weight (RW) of the composites. The T_i was determined as the temperature at the weight loss of 5 %. The weight loss due to thermal degradation of the composites occurred in two distinctive steps. The first step which occurred at 200–350 °C was mainly caused by the thermal degradation of BP. The three major constituents of BP were hemicelluloses, lignin, and cellulose, which all had lower thermal stability and degradation temperature than the matrices. The second step of weight loss was seen at 350–550 °C, which was mainly attributed to the thermal decomposition of PP and HMSPP. The composites did not lose weight anymore at temperatures higher than 600 °C.

As shown in Table 1, the 1 % TL-treated composites showed a higher value of T_i and bigger RW value compared to the untreated composite. However, the T_m and T_d at varying weight loss for the 1 % TL-treated composite were slightly lower than those of the untreated composite. Overall, TL slightly promoted the improvement of thermal stability of the BP/PP foaming composites. The improved thermal stability of TL-treated composites resulted from stronger interfacial action between the fillers and matrices and the improved mechanical strengths arising from the addition of TL.

3.5 ESEM analysis

Tensile fracture micrographs of the specimens were investigated using ESEM, and the results are presented in Fig. 5. Clearly, the interfacial adhesion between the fillers and the matrices of the untreated composite was poor and the interface was considerably clear (Fig. 5a). Meanwhile, some BP particles agglomerated into bundles and were unevenly distributed throughout the matrices and these defects caused stress concentrations and contributed to the

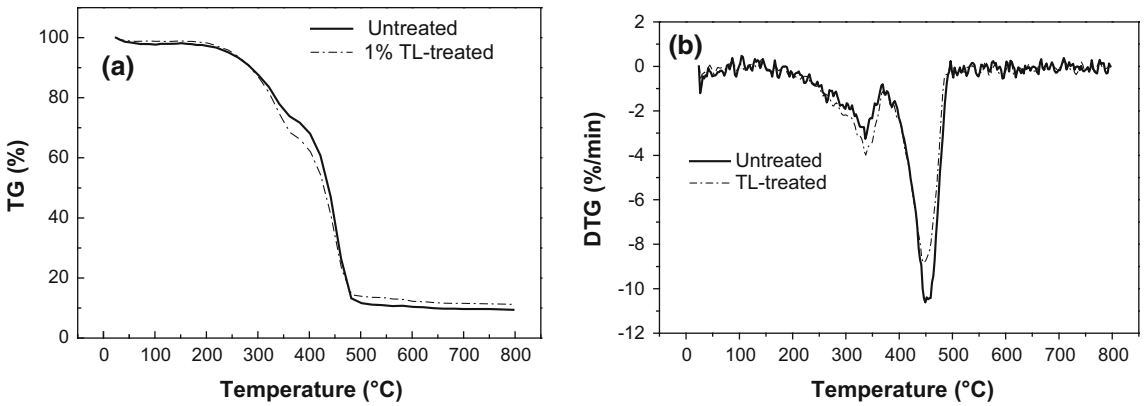

Fig. 4 Thermo-decomposition behavior of bamboo powder/PP foaming composites

Table 1 Thermal properties of bamboo powder/PP foaming composites

Sample	T_i/°C	T_m^a/°C	T_m^b/°C	W_m^a/% min^{-1}	W_m^b/% min^{-1}	T_d/°C at different weight loss				RW/% at 800 °C
						20 %	40 %	60 %	80 %	
Untreated	245	336	449	3.3	10.6	333	423	448	470	9.4
1 % TL treated	249	337	445	4.0	8.9	327	409	442	466	11.2

T_m^a, value for 1st step; T_m^b, value for 2nd step; W_m^a, maximum weight loss rate for 1st step; W_m^b, maximum weight loss rate for 2nd step

lower mechanical strengths in the untreated composite. Moreover, in some parts of the untreated composite, no matrices coated the BP surfaces (Fig. 5b). In case of the 1 % TL-treated composite, the immiscibility of the fillers and matrices was weakened drastically and the microstructure of the failure surface was much rougher (Fig. 5c). Additionally, the dispersion of BP in the matrices was improved and the interfacial boundary became indistinct (Fig. 5d). These results further confirmed that TL can improve the BP dispersion and interfacial compatibility of BP/PP foaming composites. However, partial agglomeration of BP was still observed for the TL-treated composite, which might be responsible for the insignificant improvement of mechanical properties. Therefore, improving the dispersion of the BP needs to be further studied.

3.6 FTIR study

Figure 6 presents the FTIR spectra obtained for TL, BP before and after TL modification, and the untreated and TL-treated composites. The FTIR spectrum of TL (Fig. 6a) showed a broad band at 3,378 cm^{-1} for a –OH stretching vibration, and the bands at 2,925 and 2,854 cm^{-1} are ascribed to the asymmetric stretching vibration of methyl and methylene groups, respectively. The peak at 1,739 cm^{-1} is indicative of C=O stretching due to the "bridging" structure (Fig. 7) (Li et al. 2009). The characteristic peak at 1,621 cm^{-1} is attributed to aluminium and zirconium atom with carboxyl (Freischmidt and Michell 1991). The peak at 1,466 cm^{-1} is attributed to the scissoring vibration of methylene or the symmetric deformation of methyl group. The peaks at 1,380 and 1,376 cm^{-1} are due to the symmetric stretching vibration or bending vibration of $–CH_3$. The peak at 1,078 cm^{-1} is related to C–O stretching. The peak at 611 cm^{-1} is assigned to the symmetric stretching mode of Al–O bond (Li et al. 2013). The FTIR spectrum of the untreated BP (Fig. 6b) showed the presence of bands at 3,403 cm^{-1} for –OH stretching, at 2,915 cm^{-1} for –CH stretching, at 1,601 and 1,510 cm^{-1} for C=C aromatic ring, and at 1,052 cm^{-1} for C–O stretching. Compared to the untreated BP, the TL-treated BP (Fig. 6c) exhibited new peaks at 1,741 cm^{-1} for C=O stretching, and at 1,463 cm^{-1} for –CH vibration, and at 611 cm^{-1} for Al–O vibration, which confirmed the etherification of the BP hydroxyl groups and TL groups (Fig. 7). Additionally, the intensity of –OH stretching peak was strengthened and the corresponding peak shifted from 3,403 to 3,431 cm^{-1}. Meanwhile, the peaks at 2,915, 1,601, 1,510, and 1,052 cm^{-1} were correspondingly shifted to 2,923, 1,604, 1,514, and 1,050 cm^{-1}, which further confirmed that TL can react with the hydroxyl groups of BP to form new chemical bonds (Deka and Maji 2010). Figure 6d, e show the FTIR spectra of untreated and 1 % TL-treated composites. In the TL-treated composite, new

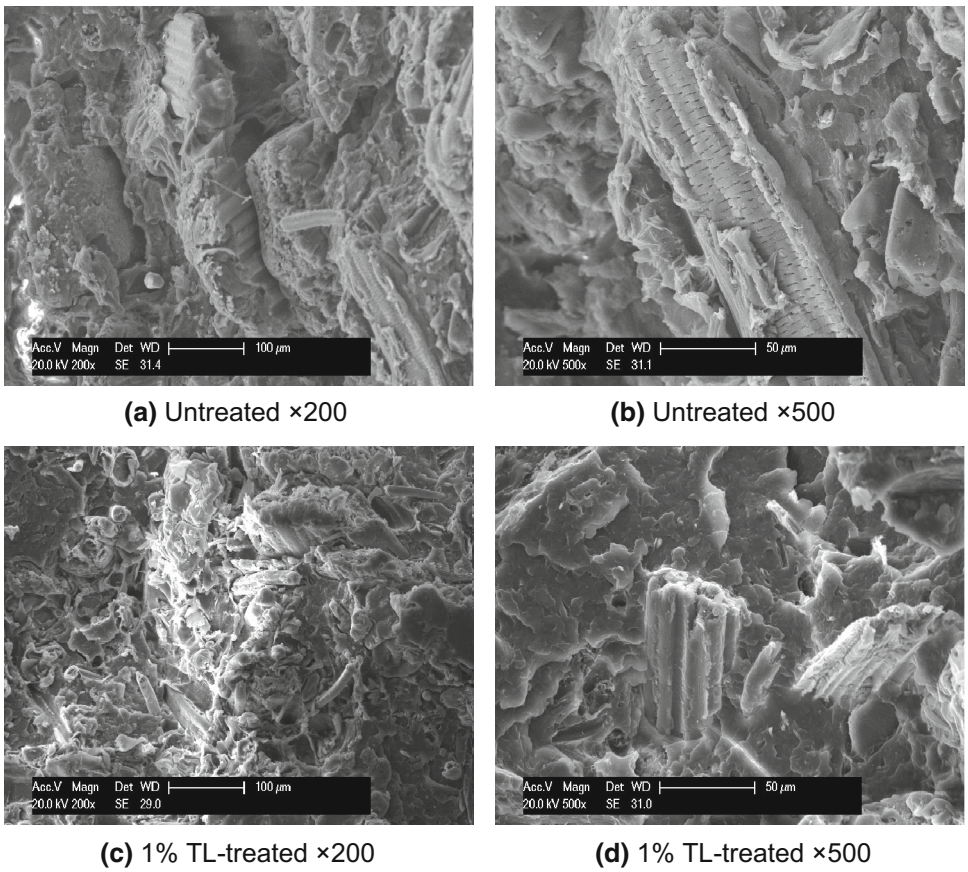

Fig. 5 ESEM micrographs of foaming composites

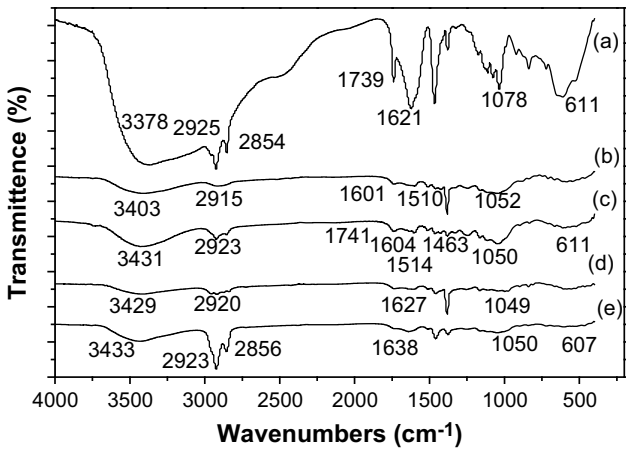

Fig. 6 FTIR spectra of the bamboo powder and composites: **a** TL, **b** BP, **c** 1 %TL-treated BP, **d** untreated composite, **e** 1 % TL-treated composite

peaks appeared at 2,856 cm^{-1} for –CH stretching of the modifying hydrocarbon and at 607 cm^{-1} for Al–O. The intensity of –OH stretching (Fig. 6e) was weakened and the corresponding peak shifted from 3,429 cm^{-1} (Fig. 6d) to 3,403 cm^{-1} (Fig. 6e). The spectral shifting from higher to lower wave number confirmed that hydrogen bonds were

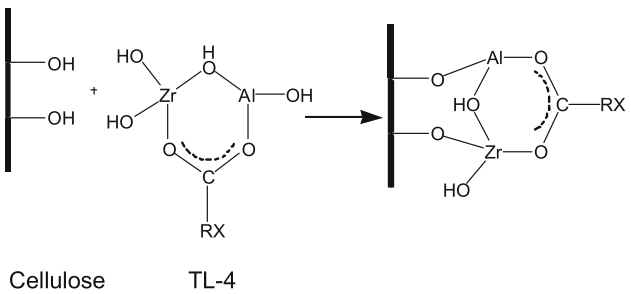

Fig. 7 Etherification reaction of cellulose hydroxyl of bamboo powder and the groups of zircoaluminate coupling agent (TL)

generated as ether linkage between BP and matrices. The intensity of –CH stretching (Fig. 6e) was increased and shifted from 2,920 cm^{-1} (Fig. 6d) to 2,923 cm^{-1} (Fig. 6e). Similar trends of shifting of hydroxyl group to lower wavenumber and increased intensity of –CH stretching were reported in the FTIR analysis of the PP/MAPP/wood composite (Awal et al. 2010). The intensity of C–O stretching was increased and shifted from 1,049 cm^{-1} (Fig. 6d) to 1,050 cm^{-1} (Fig. 6e). In conclusion, TL proved to have undergone an etherification reaction or hydrogen bonding with the hydroxyl groups of the BP at

Table 2 Elemental composition and relative amount of carbon-to-oxygen bonds on composite surfaces

Sample	Elemental composition (%)							
	C1 s					O1 s		N1 s
	C1 (C–C or C–H)	C2 (C–O)	C3 (O–C–O or C=O)	C4 (O–C=O)	$C_{ox/unox}$	O1 (C=O)	O2 (C–O)	
Untreated	58.38	16.54	6.79	0	0.40	8.59	7.86	1.84
1 % TL-treated	59.94	17.71	9.95	3.96	0.53	6.34	1.10	1.0

one end and the fatty acid or methacryloxy groups of the TL make the BP surfaces more compatible with the matrices at the other end, and thereby enhanced the interfacial bonding between BP and PP, improving the mechanical properties of composites.

3.7 XPS analysis

Table 2 shows that the elements of the composite surfaces were mostly carbon, followed by oxygen, and finally nitrogen (less than 2 %). Noticeably, the bond forms of carbon were primarily C1, followed by C2, and finally C3 or C4. The XPS data revealed that in the 1 % TL-treated composite, the C content of 1 % TL-treated composite increased from 81.71 to 91.56 %; on the contrary, the O content decreased. This was due to the chemical reaction and physical absorption of TL. Clearly, the addition of 1 % TL resulted in the relative amount of C3 representing O–C–O or C=O, a slight decrease in C2, and an obvious decrease in C1; and the appearance of a new bond type of C4 representing O–C=O. The $C_{ox/unox}$ of TL-treated composites was higher than that of the untreated one, with an increase from 0.40 to 0.53. The increased relative amount of C3, the emergence of C4, and the increased $C_{ox/unox}$ were attributed to the introduction of TL, suggesting that the chemical reaction occurred between TL and BP (Fig. 7).

Table 2 also illustrates an obvious decrease in the content of O2, representing C–O, relative to O1 of C=O. Additionally, the O1/O2 ratio was increased from 1.09 in the untreated composite to 5.76 in the TL-treated composite. As reported, the relative contents of O1 and O2 can be regarded as the areas of crystallization and amorphousness, respectively (Di and Gao 2010). Therefore, the results indicated that the crystallinity of the TL-treated composite was increased to some extent, which also accounted for the improvement of the mechanical properties and water resistance in the treated composites.

4 Conclusion

The mechanical properties and water resistance of the TL-treated bamboo powder/PP foaming composite were improved and the optimum content of TL was 1 %. The flexural modulus and bending, tensile, and notched impact strengths were enhanced by 9.0, 9.0, 9.7, and 16.2 %, respectively, and the water absorption reduced from 8.85 to 2.61 %, compared to the untreated composite. The rheological results indicated that the 1 % TL-treated composite displayed better processing properties and higher degree of homogeneity. The TG results revealed that the thermal stability of the 1 % TL-treated composite was slightly improved because the T_i increased by 4 °C.

ESEM results give evidence that the interfacial compatibility of the TL-treated composite and the dispersion of BP improved. FTIR and XPS analysis confirmed the etherification between groups of TL and hydroxyl groups of BP.

Acknowledgments This work is supported by the Twelfth Five-Year National Science and Technology Program "Research on weather-resistant and mould-proof of bamboo–plastic composites" (2012BAD54G01). Also, the authors appreciate the generous financial support of China Scholarship Council (CSC).

References

Ashori A, Nourbakhsh A (2011) Preparation and characterization of polypropylene/wood flour/nanoclay composites. Eur J Wood Prod 69(4):663–666

Awal A, Ghosh SB, Sain M (2010) Thermal properties and spectral characterization of wood pulp reinforced bio-composite fibers. J Therm Anal Calorim 99:695–701

Bledzki AK, Zhang WY, Omar F (2005) Microfoaming of flax and wood fibre reinforced polypropylene composites. Eur J Wood Prod 63(1):30–37

Chen JZ, Feng LX, Zhao YN (2006) Retention effect of cationic aluminum zirconium coupling agents. China Pulp Pap 25(5):16–19

Cohen LB (1985) Aluminum zirconium metal-organic complexes useful as coupling agents. Patent US:4,539,049

Deka BK, Maji TK (2010) Effect of coupling agent and nanoclay on properties of HDPE, LDPE, PP, PVC blend and *Phargamites karka* nanocomposite. Compos Sci Technol 70(12):1755–1761

Di MW, Gao ZH (2010) Modern analytical techniques for biomass material, 1st edn. Chemical Industry Press, Beijing, pp 78–79

Dominkovics Z, Dányádi L, Pukánszky B (2007) Surface modification of wood flour and its effect on the properties of PP/wood composites. Compos Part A 38(8):1893–1901

Dorri GM, Gray DG (1978) The surface analysis of paper and wood fibers by Esca-electron spectroscopy for chemical analysis–I. Applications to cellulose and lignin. Cell Chem Technol 12:9–23

Freire CSR, Silvestre AJD, Neto CP, Belgacem MN, Gandini A (2006) Controlled heterogeneous modification of cellulose fibers with fatty acids: effect of reaction conditions on the extent of esterification and fiber properties. J Appl Polym Sci 100(2):1093–1102

Freischmidt G, Michell AJ (1991) Performance of zircoaluminate coupling agents in wood flour/fiber-polyolefin composite. Polym Int 24(4):241–247

Gao H, Xie YJ, Ou RX, Wang QW (2012) Grafting effects of polypropylene/polyethylene blends with maleic anhydride on the properties of the resulting wood–plastic composites. Compos Part A 43(1):150–157

Guo B, Yin P, Xu J, Yi FC, Dai Y, Gao Y, Guo FQ (2011) Effect of lauric acid-based Al–Zr coupling agent on the surface modification of long afterglow phosphors. Pigment Resin Technol 40(2):100–104

Kim HS, Lee BH, Choi SW, Kim S, Kim HJ (2007) The effect of types of maleic anhydride-grafted polypropylene (MAPP) on the interfacial adhesion properties of bio-flour-filled polypropylene composites. Compos Part A 38(6):1473–1482

Lee SH, Wang SQ, Pharr GM, Xu H (2007) Evaluation of interphase properties in a cellulose fiber-reinforced polypropylene composite by nanoindentation and finite element analysis. Compos Part A 38(6):1517–1524

Lee YH, Kuboki T, Park CB, Sain M (2011) The effects of nanoclay on the extrusion foaming of wood fiber/polyethylene nanocomposites. Polym Eng Sci 51(5):1014–1022

Li B, Li YM, Yang WL (2009) Synthesis and application of zircoaluminate coupling agent as surface modifier of nano-sized titanium dioxide. J South China Univ Technol Nat Sci Ed 37(6):7–12

Li B, Mou HY, Li YM, Li YH (2013) Synthesis and thermal decomposition behavior of zircoaluminate coupling agents. Ind Eng Chem Res 52(34):11980–11987

Lou CW, Lin CW, Huang CH, Hsieh CT, Lin JH (2013) Compatibility and mechanical properties of maleicanhydride modified the wood–plastic composite. J Reinf Plast Compos 32(11):802–810

Okubo K, Fujii T, Yamamoto Y (2004) Development of bamboo-based polymer composites and their mechanical properties. Compos Part A 35(3):377–383

Rawi NFM, Jayaraman K, Bhattacharyya D (2013) A performance study on composites made from bamboo fabric and poly (lactic acid). J Reinf Plast Compos 32(20):1513–1525

Tang YJ, Li YM, Hu DW (2007) Modification, surface structure and rheological behavior of nanosized $CaCO_3$. Acta Chim Sin 65(20):2291–2298

Xie YJ, Hill CAS, Xiao Z, Militz H, Mai C (2010) Silane coupling agents used for natural fiber/polymer composites: a review. Compos Part A 41(7):806–819

Yeh SK, Kim KJ, Gupta RK (2013) Synergistic effect of coupling agents on polypropylene-based wood–plastic composites. J Appl Polym Sci 127(2):1047–1053

Zhang YC, Wu HY, Qiu YP (2010) Morphology and properties of hybrid composites based on polypropylene/polylactic acid blend and bamboo fiber. Bioresour Technol 101(20):7944–7950

Zhang ZX, Zhang J, Lu B, Xin ZX, Kang CK, Kim JK (2012) Effect of flame retardants on mechanical properties, flammability and foamability of PP/wood–fiber composites. Compos Part B 43(2):150–158

Zhou XX, Lin QJ, Chen LH (2012) Effects of the chemical foaming agents on mechanical properties and rheological behavior of the bamboo powder/polypropylene foaming composite. BioResources 7(2):2183–2198

Zhou XX, Yu Y, Lin QJ, Chen LH (2013) Effects of maleic anhydride-grafted polypropylene (MAPP) on the physico-mechanical properties and rheological behavior of bamboo powder-polypropylene foamed composites. BioResources 8(4):6263–6279